ULTRASONIC DETERMINATION OF THREE-DIMENSIONAL SPATIAL AND TEMPORAL THERMAL DISTRIBUTION FOR THERAPY MONITORING

Ajay Anand, David Savéry, Christopher S. Hall

Philips Research North America

ABSTRACT

Thermal therapies such as radio frequency, heated saline, and high-intensity focused ultrasound ablations are often performed sub-optimally due to the inability to monitor the spatial and temporal distribution of delivered heat and the extent of the necrotic tissue. Ultrasound imaging can be used to measure the deposition of heat through local thermally related changes in speed of sound; however the clinical applicability of these techniques have been hampered by the two-dimensional nature of traditional ultrasound imaging. In this paper, we present methodology, results, and validation of an imaging technique that uses a three-dimensional ultrasound imaging system to track the spatial and temporal evolution of heat deposition.

1. INTRODUCTION

The use of thermal therapies has been rapidly increasing in the fields of interventional cardiology and radiology. From the emergent techniques of radio-frequency ablation of conduction pathways in the heart for treating arrhythmias and the ablative procedures for treating focal primary and secondary liver cancer [1] to the more nascent treatments using high intensity focused ultrasound, the need for careful monitoring of the exposure of tissue to heat is a necessary component of ensuring effective treatment. Several temperature-monitoring techniques have been used historically including the use of thermocouples mounted on the end of the radio-frequency needle to spatial monitoring with magnetic resonance imaging. For practical clinical applications, these methods have been limited by either limited spatial sampling (thermocouples) or by cost of the procedure (MRI). In this paper, we will describe a technique for estimating the three-dimensional spatial extent of temperature rise using ultrasonic imaging.

The use of ultrasound to monitor temperature rise in human tissue has been the subject of much previous research [2, 3]. Ultrasound temperature monitoring is enabled by the physical observation that the speed of sound in tissue varies substantially with temperature. This variation is essentially linear and its relative sensitivity is on the order of 10^{-3} $^{o}C^{-1}$ over the range from body temperature to the realm of hyperthermia. This increase in the speed of sound (for tissues with high water content) has the effect of causing pulsed echoes to return sooner, leading to an apparent shift or equivalently an apparent movement of speckle in the tissue as viewed on an ultrasonic image. This apparent motion can then be measured to determine variations in the speed of sound and to map the increase in temperature.

Technical challenges have limited the ability to use ultrasound as a viable alternative to existing techniques for measuring temperature *in vivo*. One of these challenges is that ultrasound has historically made measurements of tissue in cross-sectional (2-D) planes. Unfortunately, temperature deposition does not only get applied in a 2-D plane, which leads to a measured apparent motion under-estimating the true change due to the heating. Moreover, significant degradation of the estimates of apparent motion is also encountered in abdominal organs as liver, where centimetric out-of-plane displacements are observed over cardiac and breathing cycles. By introducing the ability to measure ultrasonic signals from a volume instead of a plane, it is possible to detect and often correct for the undesirable motion.

In this paper, we will describe a method to determine the three-dimensional spatial distribution of temperature using a two-dimensional ultrasonic array to obtain real-time volumetric measurements. We will present the data reduction technique for estimating temperature from experimental measurements of ultrasound backscatter in a tissue-mimicking phantom, and confirmation with a gold standard.

2. METHODS

2.1 Estimation of temperature from ultrasound backscatter

2.1.1 Notion of temperature-induced strain

When a region of tissue is heated, the resulting temperature rise results in variations in the speed of sound and tissue thermal expansion. As a result, the backscattered ultrasound echoes from the heated region undergo time shifts (since the ultrasound receiver assumes a constant speed of sound throughout the medium), and these time shifts can be

mapped into *apparent displacements* assuming a nominal sound speed (typically 1540 m/s). For temperature rises up to 10 ºC, the effect of thermal expansion can be ignored [2, 4].

It has been previously shown that the measured *apparent displacements* are related to the temperature change by the following equation [2, 5]:

$$\alpha_c \Delta T = -\frac{du(z)}{dz}, \quad (1)$$

where ΔT represents the temperature change, *u(z)* represents the profile of the *apparent displacement* measured along the direction of propagation of the ultrasound beam (*z)* and α_c represents the coefficient of thermal dependence of sound speed in units of $ºC^{-1}$. The dimensionless quantity d*u(z)*/dz is referred to as *temperature-induced strain* as it is the spatial gradient of an apparent displacement.

The temperature-induced strain is measured from the ultrasound radio-frequency (RF) backscatter data acquired during the heating experiment as described in detail in the next section.

2.1.2 Temperature- induced strain estimation algorithm

The apparent displacements *u(z)* are estimated by tracking the ultrasound echo shifts between corresponding ultrasound scan lines on a pair of 3D RF data frames (one acquired before and the other acquired during heating or cool down) using techniques similar to those employed in the field of elastography [6].

Specifically, the scan RF lines are divided into a series of segments of length 3 mm with 60% overlap. For each segment, a 1-D cross-correlation algorithm is used to find the best match for this segment within a search region defined around the same spatial location on the line acquired later in time. The time shift within the search region for which the best match is obtained is referred to as the estimated *travel time change* for the segment. This procedure is repeated for all the segments in a frame to obtain a 3D travel time change map corresponding to two successive time increments. Finally, by repeating this procedure for consecutive pairs of frames, 3D maps of the travel time changes are computed for the whole experiment. These travel time change maps are scaled by 1540/2 m/s to obtain apparent displacement*s u(z)*.

The apparent displacements are finally differentiated along *z* using a least squares estimator [7] with a kernel length of 7 samples (7.2 mm) and are scaled in agreement with Eq. (1) to obtain 3D maps of the *temperature rise*.

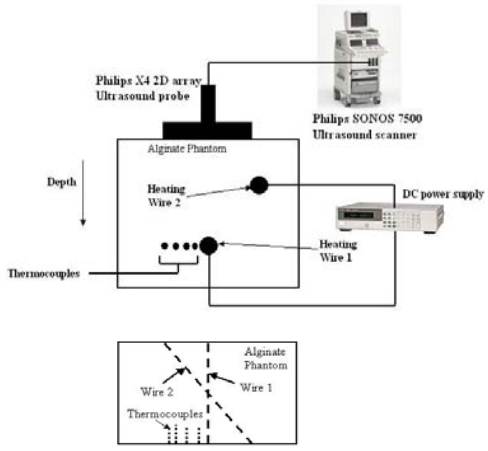

Figure 1 *(top panel)* Schematic diagram of experimental setup. *(bottom panel)* Top view of phantom setup. The phantom dimensions are 14×9×6 cm.

2.2 Experimental Setup

2.2.1 Noninvasive Ultrasound Temperature Estimation

Figure 1 shows a schematic of the experimental setup. The experiments are performed using an alginate-based phantom material. The phantom is prepared by mixing 32 g of alginate powder in 600 ml water, and poured into a mold containing two positioned conducting wires (diameter 1 mm, resistance 0.014 Ω/cm) and four pre-positioned thermocouples (Omega Inc, Stamford, CT, USA). A real-time 3D imaging ultrasonic imaging probe (X-4 on a SONOS 7500 ultrasound scanner, Philips Medical Systems, Bothell, WA) is placed in contact with the phantom and positioned to include both wires in the field of view. As shown in Figure 1(lower panel), one of the wires is placed parallel to the sides of the phantom while the other is inclined. The radial distance between each of the thermocouples and wire 1 was measured from B-mode images acquired before heating commenced.

A current of 5.7 A is applied to the wires using a DC power supply (HP 6631B, Agilent Technologies, Palo Alto, CA). The thermocouple output is digitized using a data acquisition and switch unit (Agilent 34970A). Beamformed ultrasound RF data are captured using a custom software program (AFLink, Philips Medical Systems). The entire data acquisition operation is controlled from a PC via a customized program developed using LabVIEW™ (National Instruments, Austin, TX). The total heating time is 90 seconds. The thermocouple data are sampled once every second for a period of 2 minutes, and RF data acquisition lasts 95 seconds with a 3D data frame acquired every 5 seconds. Data are then stored and processed offline in MATLAB™ (Mathworks, Natick, MA). The experiment

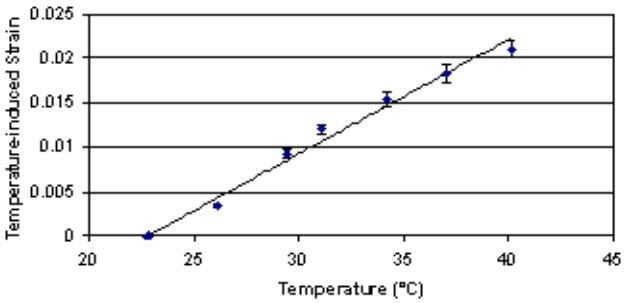

Figure 2 Plot of temperature-induced strain as a function of temperature. The slope of the linear fit provides α_c.

is performed for the parallel wire (wire 1) heated first and then both wires heated together.

2.2.2 Thermal dependence of the speed of sound

The thermal dependence of the speed of sound of the phantom material is determined through an independent calibration experiment. The phantom is placed in a heated water bath. The temperature within the bath is actively controlled by a temperature controlled water circulation system (Neslab EX-10, Thermo Electron Corporation, Waltham, MA) and monitored via thermocouples placed in and around the phantom. An ultrasonic transducer (15-6L, Philips Medical Systems) is placed on the phantom in contact with its top surface. The water bath is heated in increments of 1 to 3 ºC, and at each temperature increment RF data are acquired using the SONOS 7500 ultrasound scanner to compute the *temperature-induced strain*. The slope of the linear fit (assuming zero intercept) between the measured temperature values and the strain values gave an estimate of α_c.

3. RESULTS

Figure 2 is a plot of temperature-induced strain as a function of temperature. The estimated α_c was 0.0013 $ºC^{-1}$. In Figure 3, ultrasound derived temperatures at four radial distances (1.6, 5.6, 10 and 12 mm respectively) from the center of wire 1 are shown. At each of these radial distances, a thermocouple was placed and the measured readings are illustrated in Figure 3 as solid lines. The errors of the ultrasound derived temperature measurements are characterized by including all points at a specified radial distance along the long axis of the wire. The root mean square error between the thermocouple readings and the ultrasonically derived temperature estimates at the thermocouple locations are 0.4, 1.3, 0.3 and 0.1 ºC respectively.

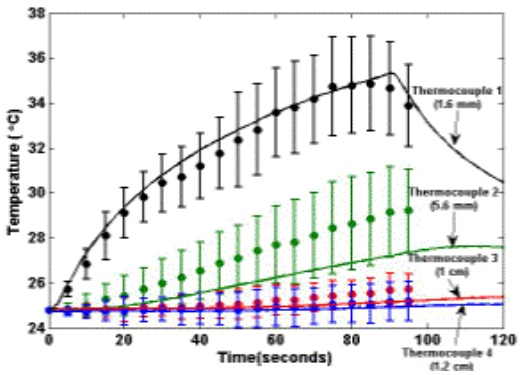

Figure 3 Ultrasonically derived temperature estimates (•) and corresponding thermocouple readings (solid line) as a function of time during heating and cool down for wire 1 heating experiment. The error bars represent the standard deviation in the ultrasound estimate.

Temperature profiles as a function of radial distance from the center of the heating wire at different times during the experiment are shown in Figure 4. The error bars at each radial location represent the standard deviation derived by including all the points along the long axis of the wire. The solid lines represent a Gaussian fit to the estimated temperature values based on a heat transfer model as proposed by Pernot et. al. [8].

The panels of Figure 5 show the three-dimensional distribution of temperature for the parallel heating wire, and the measurements with both wires heating at the same time in a second set of experiments. The displayed panels show the iso-thermal surface at 42 ºC with a cut-away showing the temperature within the volume.

4. DISCUSSION

We have shown in a phantom based experiment the feasibility of measuring three-dimensional ultrasound temperature maps. This technique holds promise for extension to *in vivo* applications for the measurement of the spatial extent of a lesion formed by various forms of thermal treatments, especially ablation procedures. To the best of the knowledge of the authors, this work represents the first demonstration of 3D spatial and temporal ultrasound thermometry.

In our simple phantom consisting of a single parallel wire, we show in Figure 3 that we obtain both accurate and precise measurements of temperature when compared to direct measurements of temperature with embedded thermocouples. The overall accuracy of our ultrasound measurements was 1.1 ºC. These values were calculated by looking at all time points and spatial locations of the thermocouples.

As with any experimental design, there were limitations to the conclusions that can be derived from our

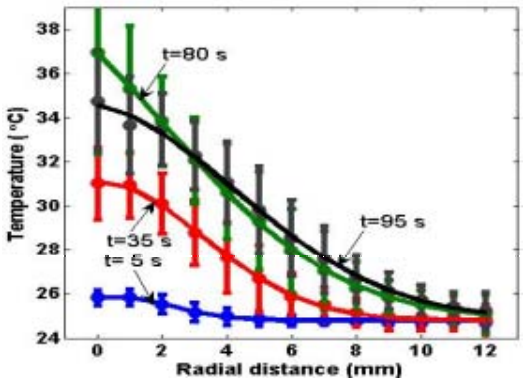

Figure 4 Temperature profiles as a function of radial distance at t=5,35,80 s (heating phase) and 95 s (cool–down phase) during the single wire (wire 1) heating experiment.

measurements. The use of a wire as the thermal source may limit the accuracy of thermally related time-shifts of signals distal to the wire because of multiple reverberations within the wire, and associated acoustic shadowing. In our measurements, we also observed that in planes where the acoustic insonification was perpendicular to the wire, we were less likely to obtain accurate measurements of temperature. Figure 3 shows a marked difference in the ultrasound-measured temperature at thermocouple position 2. This may be due to several reasons including misregistration of the thermocouple with the heating source. Experimental determination of the specific location of the thermocouples was difficult and performed under ultrasound guidance, but may have an associated error as large as 1 mm. For example, the mean square error between the ultrasound estimates at a radial distance of 6.5 mm and the thermocouple measurements at position 2 decreased to 0.4 ºC (compared to 1.3 ºC at 5.5 mm).

Our data reduction techniques could also introduce errors in the comparison of ultrasound-derived temperatures to thermocouple measurements. In particular, the use of all ultrasound-derived temperatures at a specific distance from the wire (as shown in Figure 3) assumes accurate identification of the center of the wire, and a cylindrically symmetric heating pattern that might not be completely valid due to heterogeneities in the phantom.

Some substantial technical hurdles remain before this technique can be brought to the level necessary for clinical utility. In particular, the need for compensating for gross-scale actual motion within the image that might be associated with breathing, cardiac or intestine-movement, or transducer movement still remains. This is challenging, as the gross-scale motion is much larger than the apparent motion due to heat deposition. Being able to image spatial volumes rather than 2D cross-section is undoubtedly a crucial step to truly achieve motion compensation. The development of 3D techniques for addressing these problems is a current subject of research.

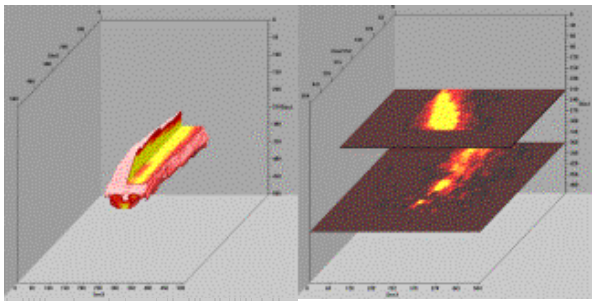

Figure 5 (left) 3D spatial temperature distribution for wire 1 only as heat source and **(right)** both wires heating simultaneously.

In conclusion, the addition of a third dimension to the spatial distribution of temperature should provide utility to the clinician as he/she can track the temperature rise near anatomical structures that might not be easily monitored in a single two-dimensional cross-section, thereby preventing unwanted thermal treatment next to sensitive tissue. In addition, the ability to observe out of plane motion due to the thermal change in speed of sound is available with real-time volumetric imaging.

Acknowledgements :- The authors wish to thank Jose Azevedo and McKee Poland for help with the experimental setup and RF data acquisition.

5. REFERENCES

[1] Garcea G., Lloyd TD. , Aylott C., Maddern G. , and B. DP., "The emergent role of focal liver ablation techniques in the treatment of primary and secondary liver tumours.," *European Journal of Cancer*, vol. 39, pp. 2150-64, 2003.

[2] R. Maass-Moreno and C. A. Damianou, "Noninvasive temperature estimation in tissue via ultrasound echo-shifts. Part I. Analytical model," *J Acoust Soc Am*, v. 100, 1996.

[3] R. Seip and E. S. Ebbini, "Noninvasive estimation of tissue temperature response to heating fields using diagnostic ultrasound," *IEEE Trans Biomed Eng*, v42, 1995.

[4] N. R. Miller, J. C. Bamber, and P. M. Meaney, "Fundamental limitations of noninvasive temperature imaging by means of ultrasound echo strain estimation," *Ultrasound Med Biol*, vol. 28, pp. 1319-33, 2002.

[5] C. Simon, P. VanBaren, and E. S. Ebbini, "Two-dimensional temperature estimation using diagnostic ultrasound," *Ultrasonics, Ferroelectrics and Frequency Control, IEEE Transactions*, vol. 45, pp. 1088-1099, 1998.

[6] J. Ophir, "Elastography: a quantitative method of imaging the tissue strain and elastic modulus in vivo," *Ultrasonic Imaging*, 1991.

[7]Kallel.F., "Least Squares Strain Estimator for Elastography," *UMB*, 1997.

[8] M. Pernot, M. Tanter, J. Bercoff, K. R. Waters, and M. Fink, "Temperature estimation using ultrasonic spatial compound imaging," *IEEE Trans Ultrason Ferroelectr Freq Control*, vol. 51, pp. 606-15, 2004.